Supplementary Information A: Fabrication Methods

The fabrication details are described in this section. The master pattern for the grating channel template was fabricated on a silicon wafer coated with 1 μm of photoresist (Sumitomo PFi88A7) and patterned using a chrome mask and contact lithography. The pattern was etched into silicon using CF_4 reactive ion etching (RIE), treated with silane (Sigma Aldrich trichloro(octyl)silane), and replicated at room temperature using polydimethylsiloxane (PDMS, Dow Corning) to generate the PDMS stamp. The samples were prepared by coating 100 nm thick and 1.5-1.8 μm thick photoresist. The PDMS stamp was applied to the photoresist prior to soft-baking, resulting in the imprint of the PDMS features into the photoresist surface. The resist surface was treated using oxygen plasma for 10 s to increase surface energy and facilitate colloidal assembly. Aqueous colloidal solution of monodisperse polystyrene spheres with diameters of 350, 390, and 500 nm (Polyscience Polybead Microspheres in 2.5% aqueous solution) was injected between a scanning microscope slide and the sample substrate. The slide was scanned parallel to the grating channel direction of the template for convective TDSA.

The lithographic exposures were conducted using a linearly polarized HeCd laser (Kimmon, λ = 325 nm, 50 mW), and a non-polarized mercury arc lamp with narrowband optical filters at λ = 365 and λ = 405 nm. After exposure doses ranging from 80-150 mJ/cm^2, the particles were removed by ultrasonic agitation in water for 10-30 seconds. The samples were then developed using 2.4% tetramethylammonium hydroxide (TMAH) developer solution (Microposit MF-CD-26) for 2 minutes. The samples were then cleaved and characterized using a scanning electron microscope (JEOL 6400F) at 5 keV.

Supplementary Information B: Particle Assembly Density on Template

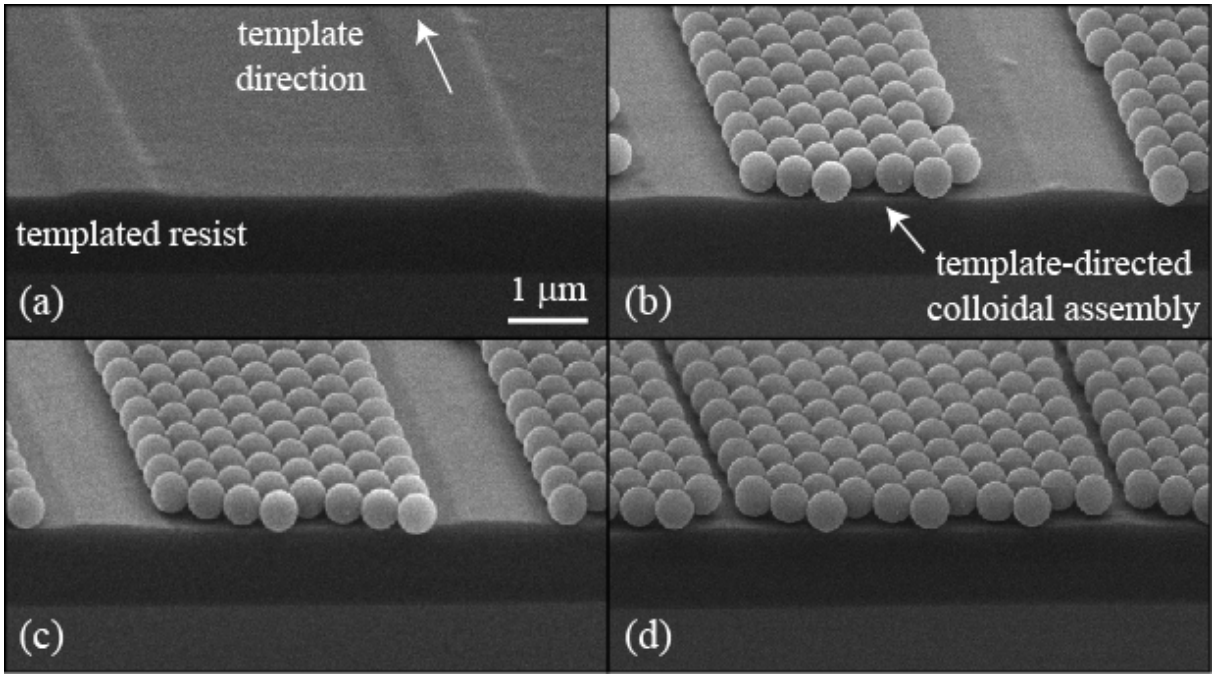

Figure S1. Cross-section micrographs of (a) the resist template after soft lithography, and results of template-directed colloidal assembly with (b) 7, (c) 8, and (d) 11 particles by controlling particle concentration during assembly.

Note given the shallow depth of the resist template, which can range from 100 to 500 nm, the template has sloped sidewalls and has a more graduate transition than other templates used for directing colloidal particle assemblies. In our case, the number of particle assembled in the template can depend on various factors, including the dimensions of the template, particle, the assembly mechanism, and the particle density. In our experiment we can control the number of particles assembled by tuning the particle concentration during convective assembly. This effect is illustrated in Figure S1, where the same resist template was use to assemble 7, 8, and 11 particles by empirically controlling for particle concentration. The precise control over the number of assembled particle through coating and evaporation speed during assembly is of significant interest, and is the subject of on-going research.

Supplementary Information C: More Fabrication Results and Lattice Analysis

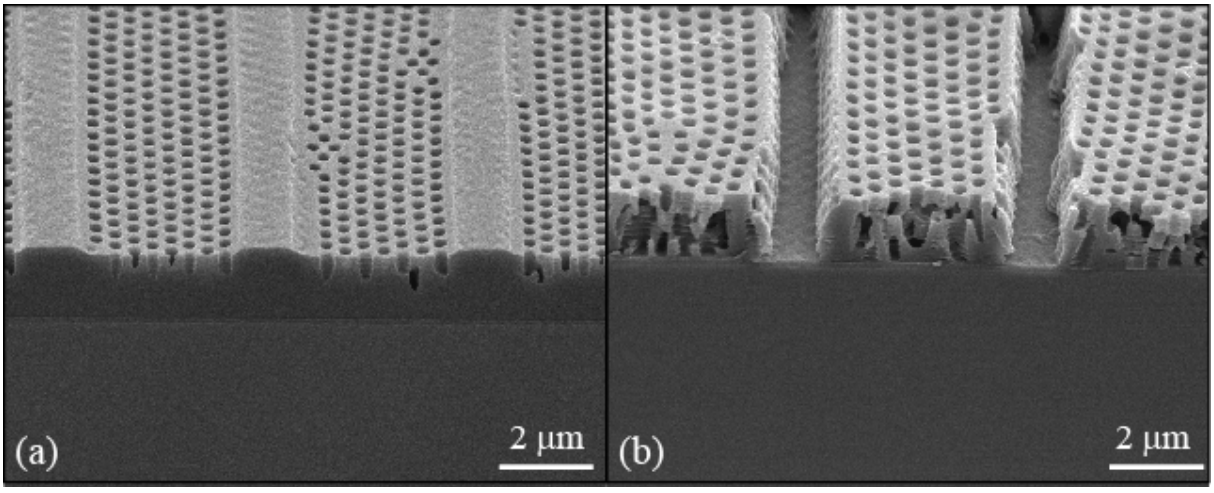

Figure S2. Hierarchical nanostructures fabricated using with particle diameter of 500 nm and light wavelength of 405 nm. (a) The structures are underexposed to show the remaining resist template. (b) Fabricated hierarchical 3D nanostructure with ridges removed.

The fabrication results of other hierarchical 3D nanostructures and their analysis are shown in this section. Figure S2 depicts structures fabricated using particle diameter of 500 nm and light wavelength of 405 nm. The structure was underexposed to investigate the transient structure formation process, as shown in Figure S2(a). It can be observed that the photochemical process is induced only on the surface, resulting in nanostructure is not fully 3D. The raised regions without particle assembly were also unexposed, resulting in the structure not being dissolved. The structure resembles a 2D photonic crystal waveguide which can be designed by controlling the microscale template geometry. Upon further exposure, the 3D nanostructures form in the region under the particle assembly and the raised regions without particles are completely dissolved, as shown in Figure S2(b).

Structures using various combinations of 500, 390, and 350 nm diameter particles and 325, 365, and 405 nm wavelengths are shown in Figure S3. Their axial periods are measured using SEM and labeled in the images. For the case with a particle size of D = 500 nm exposed to λ = 325 nm

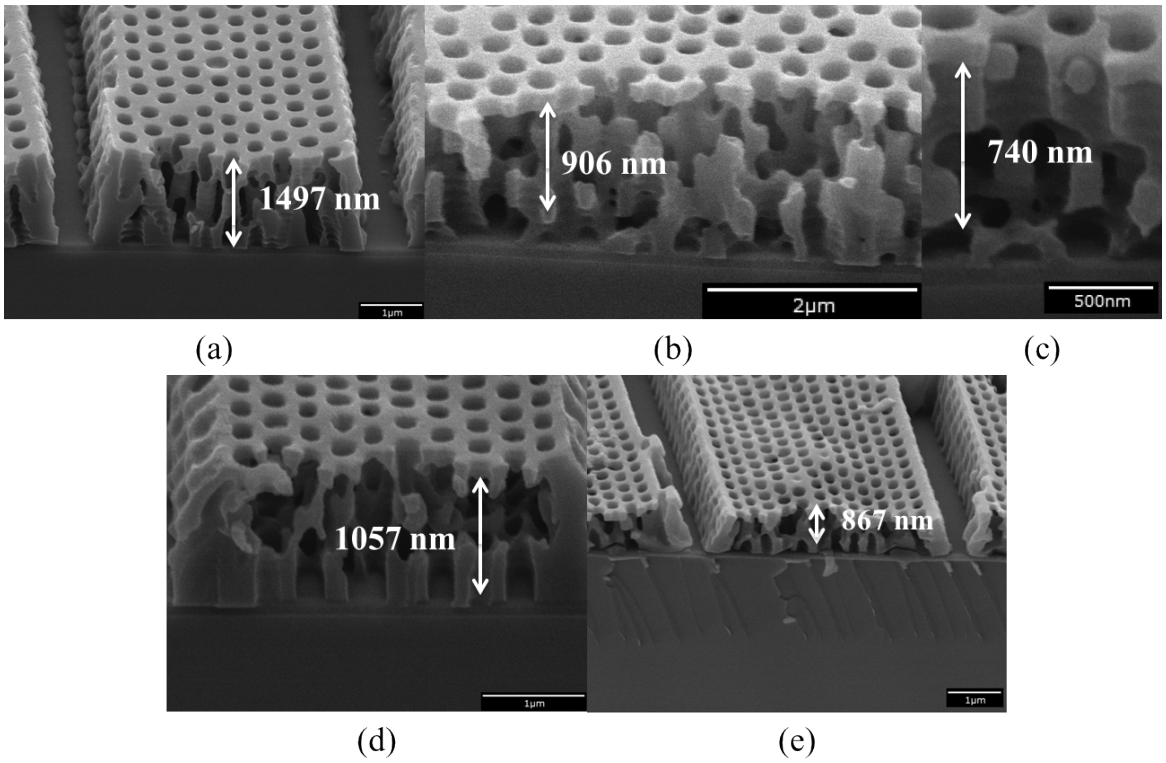

Figure S3. SEM images of cross sections for structures fabricated using (a) 500 nm spheres exposed to 365 nm UV light (120mJ/cm^2); (b) 390 nm spheres exposed to 365 nm UV light (120 mJ/cm^2); (c) 350 nm spheres exposed to 365 nm UV light (120 mJ/cm^2); (d) 390 nm spheres exposed to 325 nm UV light (118 mJ/cm^2); (e) 350 nm spheres exposed to 325 nm UV light (105 mJ/cm^2)

UV light, the axial period is greater than the maximum achievable thickness of the photoresist used. Therefore, a half axial period was measured and doubled to determine the z_t value. Greater relative size distribution for colloidal solutions with smaller diameter particles results in more assembly defects. Therefore structures fabricated using smaller particle sizes exhibit lower mechanical stability and tend to collapse.

The measured axial periods for the various fabricated samples are compared with theoretical values, as tabulated in Table S1. The analytical model was described in the main text of the

manuscript. The comparisons between the experimentally measured data and the model are plotted in Figure 5 of the manuscript.

Table S1. Comparison of measured Talbot period with theoretical model

***D* (nm)**	**λ (nm)**	**z_t predicted (nm)**	**z_t measured (nm)**	**Error (nm)**	**Percent error (%)**
350	325	853.82	867	13.2	1.5
	365	728.98	740	11	1.5
390	325	1049.62	1057	7.4	0.7
	365	905.36	906	0.6	0.1
500	325	1799.66	1790	-9.7	-0.5
	365	1576.25	1497	-79.3	-5
	405	1393.20	1390	-3.2	-0.2

Supplementary Information D: Effect of Larger Templates

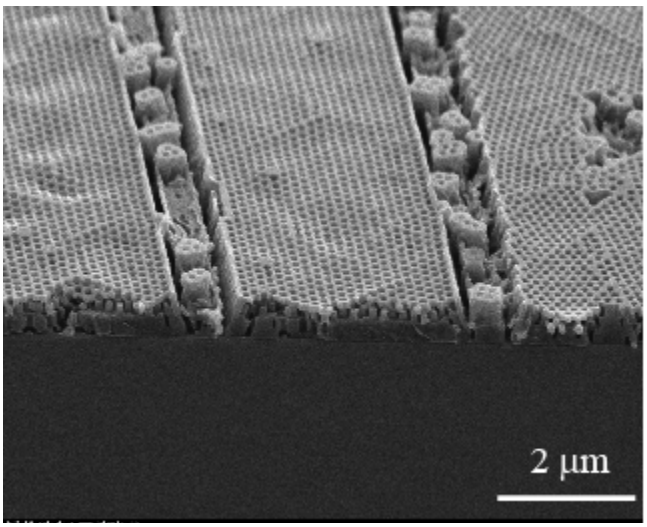

Figure S4. Fabricated hierarchical structure using larger template geometry.

Structures were also fabricated using a different 1D template to examine the effect of the microscale template. The larger template has ridge width of 2 μm and trench width of 8 μm, which is double the template size used in Figure 4. In this case particles with D = 390 nm were assembled on the template resist and exposed to λ = 365 nm UV light. The fabricated structures are shown in Figure S4, where the 3D periodic structure now spans a greater channel width of 8 μm. However, the axial period of the periodic nanostructures is measured to be 905 nm, which is the same for structures fabricated using the smaller templates. Therefore the larger channel structure width can be effectively controlled by the template geometry. Note that more defects can be observed since the template is much larger than the particle diameter and around 20 particles are guided along the template width. The raised portion of the template is also not completely free of particles, resulting in outstanding structures between the porous regions.